HHS Public Access

Author manuscript

Lab Invest. Author manuscript; available in PMC 2014 December 01.

Published in final edited form as:

Lab Invest. 2014 June ; 94(6): 623–632. doi:10.1038/labinvest.2014.52.

Genetic modulation of nephrocalcinosis in mouse models of ectopic mineralization: The *Abcc6*^{tm1Jfk} and *Enpp1*^{asj} mutant mice

Qiaoli Li[1], **David W. Chou**[1], **Thea P. Price**[1,2], **John P. Sundberg**[3], and **Jouni Uitto**[1]

[1]Department of Dermatology and Cutaneous Biology, Thomas Jefferson University, Philadelphia, PA

[2]Department of Surgery, Thomas Jefferson University, Philadelphia, PA

[3]The Jackson Laboratory, Bar Harbor, ME

Abstract

Ectopic mineralization of renal tissues in nephrocalcinosis is a complex, multifactorial process. The purpose of this study was to examine the role of genetic modulation and the role of diet in nephrocalcinosis using two established mouse models of ectopic mineralization, *Abcc6*^{tm1Jfk} and *Enpp1*^{asj} mice, which serve as models for pseudoxanthoma elasticum and generalized arterial calcification of infancy, two heritable disorders, respectively. These mutant mice, when on standard rodent diet, develop nephrocalcinosis only at very late age. In contrast, when placed on an “acceleration diet” composed of increased phosphate and reduced magnesium content they showed extensive mineralization of the kidneys affecting primarily medullary tubules as well as arcuate and renal arteries, as examined by histopathology and quantitated by chemical assay for calcium. Mineralization could also be detected noninvasively by micro computed tomography. While the heterozygous mice did not develop nephrocalcinosis, compound heterozygous mice carrying both mutant alleles, *Abcc6* $^{tm1Jfk/+}$, *Enpp1*$^{+/asj}$, developed ectopic mineralization similar to that noted in homozygous mice for either gene, indicating that deletion of one *Abcc6* allele along with *Enpp1* haploinsufficiency resulted in renal mineralization. Thus, synergistic genetic defects in the complex mineralization/anti-mineralization network can profoundly modulate the degree of ectopic mineralization in nephrocalcinosis.

Keywords

Genetic modulation of nephrocalcinosis; mineral content of nephrocalcinosis; mouse models of ectopic mineralization; the role of experimental diet in kidney mineralization

Ectopic mineralization, *i.e.*, precipitation of calcium phosphate complexes on connective tissues in aberrant locations, is a complex process encountered in a number of clinical

Address for Correspondence: Jouni Uitto, MD, PhD, Department of Dermatology and Cutaneous Biology, Jefferson Medical College, 233 S. 10th Street, Suite 450 BLSB, Philadelphia, PA 19107, Tel: 215-503-5785, Fax: 215-503-5788, Jouni.uitto@jefferson.edu.

DISCLOSURE/CONFLICT OF INTEREST

The authors declare no competing interests.

situations with considerable morbidity and mortality. Two general mechanisms of ectopic mineralization have been recognized: (a) metastatic calcification which results from elevated levels of serum phosphate and/or calcium, and (b) dystrophic calcification which occurs in tissues inflicted by an insult or injury under normal calcium and phosphate homeostasis (1). Both these forms of calcification have been clinically encountered in diseases affecting different organs, including the kidney. Nephrocalcinosis clinically refers to the presence of radiologically demonstrable calcium deposits in renal parenchyma, and it is pathologically different from crystal deposition in the lumen of the urinary collecting systems in nephrolithiasis (2, 3). Nephrocalcinosis can be divided into two distinct categories, (a) intratubular nephrocalcinosis, and (b) interstitial nephrocalcinosis, which appear to result from different pathological mechanisms. In addition to calcium phosphate deposition in kidneys, nephrocalcinosis can be caused by deposition of calcium oxalate in heritable diseases, such as autosomal recessive primary hyperoxaluria type I (4). Furthermore, conditions such as inflammatory bowel disease, complicated by short bowel syndrome, can result in significant secondary hyperoxaluria and again manifest with nephrocalcinosis and subsequent renal failure (5).

The prototype of heritable ectopic mineralization disorders in humans is pseudoxanthoma elasticum (PXE), an autosomal recessive Mendelian disorder characterized by ectopic mineralization in a number of tissues, with clinical manifestations primarily in the skin, the eyes and the cardiovascular system (6, 7). In addition to the tissues with diagnostic clinical manifestation, calcium deposition has been documented in a number of organs, including the kidneys (8, 9). This disorder is caused by mutations in the *ABCC6* gene which is expressed primarily in the liver and to a lesser extent in the proximal tubules of the kidneys (10). ABCC6 is postulated to serve as an efflux transporter in the baso-lateral surface of the hepatocyte plasma membranes, but its physiologic substrates are currently unknown (6, 7). The involvement of the vascular system in patients with PXE manifests with nephrogenic hypertension, intermittent claudication, and, occasionally, early myocardial infarcts and stroke. Another more severe form of ectopic mineralization is generalized arterial calcification of infancy (GACI), often diagnosed by prenatal ultrasound demonstration of calcification of a number of arterial blood vessels (11, 12). The affected individuals in most cases die from cardiovascular and renal complications prior to 6 months of age. GACI, also an autosomal recessive disease, is caused by mutations in the *ENPP1* gene, which encodes ectonucleotide pyrophosphatase/phosphodiesterase 1 (ENPP1), an enzyme required for conversion of ATP to AMP and inorganic pyrophosphate (PP_i) (13). Since PP_i is required for prevention of ectopic mineralization under physiological conditions, in the absence of *ENPP1* the ratio of P_i/PP_i increases allowing local precipitation of calcium phosphate to ensue. Recently, a subset of patients with GACI has also been shown to harbor mutations in the *ABCC6* gene, attesting to the genotypic overlap with PXE (14, 15).

A number of animal models have been developed to recapitulate the features of these ectopic mineralization disorders (1). Specifically, targeted ablation of the *Abcc6* gene in mice results in late-onset, yet progressive ectopic mineralization in the skin, the eyes and the cardiovascular system similar to that noted in patients with PXE (16, 17). Similarly, *Enpp1*$^{-/-}$ knockout mice as well as allelic mutant mice, such as *asj* and *ttw*, demonstrate

features resembling those seen in patients with GACI (18–20). We have recently characterized the *Enpp1*^{asj} allelic mutation as a mouse model recapitulating features of GACI, including early-onset, severe calcification of arterial blood vessels resulting in early demise of the animals (20). While the initial characterization of these mice has primarily focused on ectopic mineralization in the skin and the arterial blood vessels, in this study we have examined the features of nephrocalcinosis in *Abcc6*^{tm1Jfk}/*Abcc6* ^{tm1Jfk} (hereafter referred to as *Abcc6*$^{-/-}$) and *Enpp1*^{asj}/*Enpp1*^{asj} (hereafter referred to as *asj*) mice, with emphasis on genetic and dietary modulation of the mineralization process.

MATERIALS AND METHODS

Mice and Diet

The *Abcc6*^{tm1Jfk}/*Abcc6*^{tm1Jfk} mouse (referred to in this study as *Abcc6*$^{-/-}$ mouse), a model for PXE, was developed by targeted ablation of the *Abcc6* gene (17). *Abcc6*$^{-/-}$ mice were made congenic by backcrossing heterozygous (*Abcc6*$^{+/-}$) mice on C57BL/6J background for 10 generations. The *Enpp1*^{asj}/ *Enpp1*^{asj} (referred to in this study as *asj*) mouse, a model for GACI, was obtained from The Jackson Laboratory (Bar Harbor, ME). Wild-type, *Enpp1*$^{+/asj}$ and *asj* mice were generated from heterozygous matings on C57BL/6J background (20). Mice were maintained either on standard laboratory diet (Laboratory Autoclavable Rodent Diet 5010; PMI Nutritional International, Brentwood, MO) or fed an “acceleration diet” (Harlan Teklad, Rodent diet TD.00442, Madison, WI), which is enriched in phosphorus and has reduced magnesium content. The “acceleration diet” was previously shown to expedite the mineralization processes in *Abcc6*$^{-/-}$ mice, in comparison to the same mice kept on standard rodent diet (21, 22). For the content of the two diets, see: Regular Diet; http://www.labdiet.com/cs/groups/lolweb/@labdiet/documents/web_content/mdrf/mdi4/~edisp/ducm04_028443.pdf, and Accelerated Diet; http://www.harlan.com/online_literature/teklad_lab_animal_diets. It should be noted that neither type of diet has measurable levels of oxalate (Tina Herfel, Harlan Laboratories, personal communication).

In the first set of experiments, *Abcc6*$^{-/-}$ and *asj* mice were placed on either standard laboratory diet or acceleration diet, with 6 mice per group at 4 weeks of age. After 2 months on this diet, *Enpp1*$^{+/+}$ and *asj* mice were imaged by CT scan for evidence of tissue mineralization (20, 23). The mice were euthanized and necropsied at 3 months of age for histopathological and biochemical analysis.

In the second set of experiments, compound *Abcc6; Enpp1* transgenic mice were generated by intercrossing *Abcc6*$^{-/-}$ mice with *asj* mice. The resultant *Abcc6*$^{+/+}$*;Enpp1*$^{+/+}$, *Abcc6*$^{+/-}$*; Enpp1*$^{+/+}$, *Abcc6*$^{+/+}$*;Enpp1*$^{+/asj}$, and *Abcc6*$^{+/-}$*;Enpp1*$^{+/asj}$ mice were placed on acceleration diet, with 8–12 mice per group at 4 weeks of age. At 7 months of age, all mice were euthanized and necropsied for further analysis.

Mice were maintained under standard conditions at the Animal Facility of Thomas Jefferson University. All protocols were approved by the Institutional Animal Care and Use Committee of Thomas Jefferson University. Proper handling and care were practiced according to the animal welfare policies of the Public Health Service.

Histopathological Analysis

Left kidneys and other organs from euthanized mice were fixed in 10% phosphate-buffered formalin and embedded in paraffin. The tissues were sectioned (6 μm thick), placed onto glass slides and stained with Hematoxylin-Eosin (HE) or Alizarin Red (AR) stain using standard procedures. Slides were examined for mineralization under a Nikon (Tokyo, Japan) Te2000 microscope and an AutoQuant imaging system (AutoQuant Imaging, Watervliet, NY). The slides were also examined under polarized light with ECLIPSE LV100POL Polarizing microscope (Nikon Instruments).

EDAX Analysis and Topographic Mapping of Mineral Deposits

Sections of kidney containing mineral deposits were analyzed by energy dispersive X-ray (EDAX) analysis and topographic mapping (24). Paraffin sections were mounted onto carbon carriers, imaged and analyzed for elemental composition with a FEI 600 Quanta FEG scanning electron microscope (FEI Company, The Netherlands) fitted with an PRISM^{60} detector (Princeton Gamma-Tech, Inc., Rocky Hill, NJ, USA). X-ray topographic (RADAR) maps of calcium and phosphorus were acquired using Spirit software version 1.07.05 (Princeton Gamma-Tech, Inc.). EDAX spectra and topographic maps were collected for 120 seconds and 673 seconds (80 frames), respectively.

Chemical Quantification of Calcium Deposition

To quantify the mineral deposition in kidneys, right kidneys were harvested and decalcified with 1.0 mol/L HCl for 48 hours at room temperature. The solubilized calcium contents in these samples, as well as in serum of the same mice, were determined colorimetrically by the *o*-cresolphthalein complexone method (Calcium (CPC) Liquicolor; Stanbio Laboratory, Boerne, TX). Calcium values in kidneys were normalized to the tissue weight. Phosphate content in serum was determined with a Malachite Green phosphate assay kit (BioAssay Systems, Hayward, CA).

Inorganic Pyrophosphate Assay

PP_i was measured by an enzymatic assay using uridine-diphosphoglucose (UDPG) pyrophosphorylase as described previously (25, 26), with modifications. Heparinized plasma samples (20 μl; 1:4 dilution) were heated at 65°C for 10 min, followed by three different assays performed on each sample: (1) no addition of PP_i standard, (2) pre-incubation with 0.35 U pyrophosphatase at 37°C for 1 hour, and (3) addition of 3 μM PP_i. Samples were then added to 100 μl of reaction buffer that contained 5.2 mM Mg acetate, 57 mM Tris acetate (pH 7.8), 4 μM NADP, 7.5 μM UDPG, 18.6 μM glucose-1, 6-diphosphate, 0.14 U UDPG pyrophosphorylase, 2.5 U phosphoglucomutase, 0.4 U glucose-6-phosphate dehydrogenase, and 0.02 μCi [^{3}H]UDPG. After a 30 min incubation at 37°C, 200 μl of 4% activated charcoal was added to each sample with occasional stirring to bind residual UDPG. After centrifugation, the radioactivity in 100 μl of the supernatant was counted.

Serum Urea and Creatinine Assays

Serum levels of urea and creatinine were measured using quantitative kits, QuantiChrom™ Urea Assay Kit and QuantiChrom™ Creatinine Assay Kit (BioAssay Systems), respectively.

Immunofluorescence

Paraffin-embedded tissue sections (6 μm thick) were deparaffinized in xylene and rehydrated in descending concentrations of ethanol. Tissues were subject to antigen unmasking by boiling in citrate-based unmasking solution (Vector Laboratories, Burlingame, CA) for 15 minutes and then permeabilized with 0.1% Triton X-100 in PBS. Slides were washed in 0.1% Tween-20 in PBS (PBST), and sections were blocked with 3% bovine serum albumin in PBST for 1 hour at room temperature. After blocking, sections were incubated with primary antibody against fetuin-A (1:100; R&D Systems, Minneapolis, MN) or osteopontin (1:20; R&D Systems) overnight at 4°C. Negative controls were incubated with 3% bovine serum albumin in PBST in place of the primary antibody. Slides were washed again in PBST and incubated with Alexa Fluor 488 donkey anti-goat IgG secondary antibody (1:800; Life Technologies-Invitrogen, Carlsbad, CA) for 1 hour. Fluorescence microscopy was immediately performed using a Nikon Te2000 microscope.

Small-Animal CT

After 8 weeks on acceleration diet, wild type and *asj* mice were examined for tissue mineralization by CT scan. Briefly, mice were anesthetized with a xylazine-ketamine-acetopromazine cocktail (160 μL per 25 g body weight of 10 mg/kg xylazine, 200 mg/kg ketamine, and 2 mg/kg acetopromazine), and then scanned in a MicroCAT II system (ImTek, Oak Ridge, TN). To analyze mineralization in kidneys, a three-dimensional surface rendering was performed for each mouse using Amira version 3.1 software (Visualization Sciences Group, Burlington, MA). Ectopic calcification was also noted by scanning isolated kidneys *ex vivo*.

Statistical Analysis

The comparisons between different groups of mice were completed using the two-sided Kruskal–Wallis nonparametric test, comparable to one-way analysis of variance, but without the parametric assumptions. All statistical computations were completed using SPSS version 15.0 software (SPSS Inc., Chicago, IL).

RESULTS

Nephrocalcinosis in Mouse Models of Ectopic Mineralization

We have previously characterized *Abcc6*$^{-/-}$ and *asj* mice, which demonstrate extensive connective tissue mineralization particularly in vascular connective tissues, as animal models for PXE and GACI, respectively (17, 20). While the previous studies centered on vascular and cutaneous mineralization, we now focused on ectopic mineralization in the kidneys by histopathology, direct chemical assay for calcium content, energy dispersive X-ray analysis and computed tomography (CT) imaging.

First, histopathologic examination of *Abcc6*$^{-/-}$ and *asj* mice at the age of 3 months, when kept on standard control rodent diet, did not reveal any mineralization in the kidneys (Fig. 1a). However, if these mice were placed on an “acceleration diet” enriched in phosphate and reduced in magnesium (21, 22), acceleration of the mineralization process was observed. Extensive tubular and vascular mineralization was noted when kidney tissues were

examined by routine hematoxylin and eosin (HE) and calcium-specific Alizarin Red (AR) stains (Fig. 1b). Direct quantitative chemical assay of calcium revealed ~30-fold increase in *Abcc6*$^{-/-}$ mice and over 6-fold increase in *asj* mice, when placed on acceleration diet as compared to the mice on control diet (Fig. 1c). The mineralization affected primarily the medullary tubules as well as arcuate and renal arteries. As reported previously, wild type mice in the corresponding genetic background do not demonstrate a significant degree of mineralization in the kidneys even when placed on the acceleration diet (20, 22).

The renal mineralization of *asj* mice on acceleration diet could also be demonstrated non-invasively by micro CT-imaging, findings which correlated with the histopathological examinations (Fig. 2), and similar observations were also made on *Abcc6*$^{-/-}$ mice under identical experimental conditions (not shown). It should be noted that mineral deposition in kidneys of double heterozygous mice was accompanied by statistically significant increase in the kidney weight. Specifically, the weight of kidneys in *Abcc6*$^{+/-}$*; Enpp1*$^{+/asj}$ was 194.8±6.5 mg (mean ± SE) compared to 167.9±5.4 and 173.9±6.8 mg in *Abcc6*$^{+/-}$ and *Enpp1*$^{+/asj}$, respectively ($p<0.05$, Student's t-test; n=8–13).

The Mineral Deposits Consist of Hydroxyapatite

Energy dispersive X-ray (EDAX) analysis was used to identify the exact content of the mineral deposits (24), which by Alizarin Red stain and direct chemical assay were shown to contain calcium in afflicted kidneys of the *asj* mice. These analyses revealed that calcium and phosphorus were the principal ions in ~2:1 ratio (Fig. 3). Topographic distribution of these two ions, as examined by RADAR mapping, revealed co-localization, suggesting that the mineral deposits consist of hydroxyapatite. Immunofluorescence of the mineral deposits both in *asj* and *Abcc6*$^{-/-}$ mice revealed the presence of two mineralization associated proteins, fetuin-A (AHSG) and osteopontin (OPN), suggesting active ongoing ectopic mineralization (Fig. 4). As indicated above, nephrocalcinosis can also be caused by calcium oxalate deposition (4, 5). For this reason, the mineral deposits were also examined under polarizing light. No polarizing material suggestive of the presence of calcium oxalate in the deposits was noted.

Genetic Modulation of the Mineralization Process

To examine the role of genetic contribution to the mineralization process, *Abcc6*$^{+/-}$ and *Enpp1*$^{+/asj}$ heterozygous mice were placed on acceleration diet, and the degree of mineralization in the kidneys was examined in parallel to wild-type (*Abcc6*$^{+/+}$*; Enpp1*$^{+/+}$) and double heterozygous (*Abcc6*$^{+/-}$*; Enpp1*$^{+/asj}$) mice. When examined at 7 months of age, *i.e.*6 months after being placed on the acceleration diet, few distinct foci of ectopic mineralization were noted in wild-type or in single heterozygote mice (Fig. 5a). However, the double heterozygous mice revealed extensive mineralization in the kidneys, again associated with tubules, similar to homozygous *Abcc6*$^{-/-}$ and *asj* mice (Fig. 5a). The degree of mineralization was also documented by direct chemical assay of calcium, which revealed significantly elevated amounts of calcium in double heterozygous mice in comparison to the other groups (Fig. 5b). It should be noted that each group consisted of both male and female mice, but separate analysis within each group did not reveal statistically significant sex differences. These results indicate that inactivation of one allele of *Abcc6* when combined

with haploinsufficiency of *Enpp1* can result in extensive mineralization of the kidney, indicating synergistic, digenic modulation of the ectopic mineralization of the kidneys in mice.

Blood Parameters in Mice with Nephrocalcinosis

The mice placed on acceleration diet at 4 weeks of age were sacrificed at the age of 7 months, and the serum and heparinized plasma were collected for analysis of calcium, phosphate and pyrophosphate by chemical assays. No difference in serum calcium, inorganic phosphate or pyrophosphate concentrations was noted (Table 1). Serum urea and creatinine levels were unchanged, suggesting normal renal function in these mice despite considerable nephrocalcinosis (Table 1).

DISCUSSION

Nephrocalcinosis, characterized by aberrant deposition of calcium in the kidney parenchyma and tubules, is a complex disorder associated with a number of systemic and renal metabolic diseases, including acute phosphate nephropathy, primary hyperparathyroidism, and distal renal tubular acidosis (2, 3). The aberrant calcium deposition may be asymptomatic but can eventually lead to progressive renal failure and end-stage renal disease. Nephrocalcinosis could be considered to be a passive phenomenon resulting from deposition of a supersaturated phosphate product associated with tissue remodeling and ultimately leading to the loss of functioning renal parenchyma. It has been demonstrated that acute phosphate nephropathy can be actively modulated by inflammatory repair mechanisms, suggesting a role for regulatory T cells (27). However, the mechanistic details in many of the pathological situations resulting in ectopic calcium deposition in kidney remain to be explored.

A number of animal models have been developed to examine the pathophysiology leading to calcium phosphate crystal deposition in the renal tissues, and many of these models emphasize the role of inorganic phosphate and pyrophosphate in the disease process (2, 3). Specifically, elevated serum P_i levels can result in tissue mineralization not only in the kidneys but also in a number of other tissues, including the skin, and these changes primarily reflect the increased relative ratio of P_i/PP_i, the latter being a potent inhibitor of mineralization (28). Changes in the local pH as well as exposure to specific proteases may also modulate the crystal deposition (2, 3).

Interstitial nephrocalcinosis has been suggested to be a result of two different mechanisms: (a) translocation of intratubular crystals, and/or (b) *de novo* interstitial crystal formation. It has been proposed that the first possibility involves translocation of crystals via transcytosis, *i.e.*, internalization of small intraluminal crystals within apical vesicles, followed by transcellular translocation to the baso-lateral site and release of crystals into the interstitial extracellular milieu (2). Although apical endocytosis of small crystals has been described, there is little evidence to support the basolateral release of crystals into interstitium (29, 30). An alternative hypothesis postulates *de novo* crystal formation in the interstitium directly as a result of P_i super saturation. This appears to be primarily a physicochemical event without participation of cells as noted in active osteogenic processes. The interstitial *de novo*

mineralization can result in development of so-called Randall's plaque, and the initially formed particles are deposited on basement membranes of the thin loops of Henle (31). These particles then grow extending into the medullary interstitium and further towards the papillary surface. The mineral syncytium can lie beneath the uroepithelium and may become exposed to the urinary environment after the loss of uroepithelial integrity.

The interstitial renal mineralization can be modulated by a number of genetic factors. Uromodulin (Tamm-Horsfall protein, THP) is a kidney-specific protein synthesized in cells of the ascending limbs of the loop of Henle. This protein coats the luminal side of the epithelium, it is abundant in human urine, and it can be present in the nephrolith matrix, which has high affinity with calcium phosphate crystals (32, 33). Targeted ablation of the mouse uromodulin gene in the THP knockout mice resulted in formation of microcrystals consisting exclusively of calcium phosphate (34, 35). Induction of hypercalciuria by the administration of vitamin D3 resulted in extensive crystal deposition in the kidneys of these knockout mice. These results indicated, therefore, that uromodulin is a physiologic inhibitor of mineral deposition in the kidneys, and its absence promotes crystallization and stone formation. Another transgenic mouse model, sodium phosphate co-transporter (Npt2a) null mouse *Slc34a1*^{tm1Hten} exhibits increased urinary excretion of P_i leading to increased serum vitamin D levels and development of hypercalcemia and hypercalciuria (36). From birth, these targeted mutant mice demonstrate progressive development of renal deposits consisting of calcium phosphate. By the age of 6 months, most of these crystal deposits are located in the renal interstitium. Thus, genetic manipulation of critical proteins expression in the kidney can result in nephrocalcinosis.

In this study, we have examined nephrocalcinosis in two animal models of ectopic mineralization, *Abcc6*$^{-/-}$ and *asj* mice, both characterized by multisystem deposition of mineral crystals (17, 20). These mouse models have been extensively studied with respect to vascular mineralization (1), but little is known about the mineralization of the kidneys. Our results demonstrated extensive ectopic mineralization in both genetic mouse models when the animals were placed on an acceleration diet, which we have previously shown to accelerate the mineralization process (21, 22). This diet contains 0.85% phosphate, *i.e.*2-fold higher than in the standard mouse diet, and 0.04% magnesium, which is 20% of that in control diet (22). In fact, we and others have recently demonstrated that the magnesium content of the diet can profoundly modulate the extent of mineralization in the *Abcc6*$^{-/-}$ mice, and increasing the magnesium concentration by 5-fold over the control diet completely abolishes the mineralization process (37–39). These observations support the previous suggestions that dietary factors, particularly P_i and Mg^{2+}, can play a role in ectopic connective tissue mineralization. In addition, the acceleration diet contains 100 IU/g of vitamin D_3, while the corresponding content in the control diet is 4.4 IU/g (22).

Characterization of the mineralization process in these mice, when placed on the acceleration diet, revealed extensive mineralization in the kidney interstitium, primarily affecting the medullary tubules as well as arcuate and renal arteries. Thus, the *Abcc6* and *Enpp1* genes clearly play a role in modulating nephrocalcinosis, since wild-type mice in the corresponding genetic background do not demonstrate a significant degree of mineralization even when placed on the same diet. The mineral deposits in the kidneys of the *Abcc6*$^{-/-}$ and

asj mice were shown to consist of calcium and phosphate, and these two principal ions co-localized in the mineral deposits, suggesting the presence of hydroxyapatite crystals (Fig. 3). The importance of this observation is emphasized by the fact that mineral crystals in different mouse models have been shown to consist either of calcium phosphate or calcium oxalate (2, 3). Thus, the mineralization of renal interstitium in these mice appears to be similar to that previously demonstrated in other tissues, particularly in the dermal sheath of vibrissae and vascular connective tissues (1, 20, 24). The relevance of these mouse findings to human disease is emphasized by the observations that the mineral deposits in human kidneys in nephrocalcinosis have been shown to consist of either calcium phosphate or calcium oxalate (2, 3). In patients with PXE, kidney mineralization has been documented by ultrasound and autopsy (8, 9). In GACI, particularly in patients caused by ENPP1 deficiency, but also in those with mutations in the *ABCC6* gene, vascular mineralization in kidney has also been documented (14, 15).

The two targeted mutant mouse models, *Abcc6*$^{-/-}$ and *asj*, both develop extensive ectopic mineralization in a number of organs, but the rate of mineralization and the organs becoming predominantly affected vary. The *Abcc6*$^{-/-}$ mice develop relatively late-onset mineralization affecting the skin, the Bruch's membrane of the retina and arterial blood vessels, while *asj* mice demonstrate relatively early-onset mineralization primarily affecting the cardiovascular system (17, 20). These observations are consistent with the phenotypic manifestations in the corresponding human diseases, PXE and GACI, caused by mutations in the *ABCC6* and *ENPP1* genes, respectively (6, 7, 10–12).

PXE and GACI are autosomal recessive disorders, and the heterozygous carriers demonstrate little, if any, evidence of mineralization. Similarly, the mutations in the *Abcc6*$^{-/-}$ and *asj* mice are autosomal recessive in that the heterozygous carriers of the mutation do not demonstrate dermal or vascular mineralization (17, 20). Along with these observations, the heterozygous *Abcc6*$^{+/-}$ and *Enpp1*$^{+/asj}$ mice did not demonstrate significant mineralization in the kidneys when placed on the acceleration diet (Fig. 5). However, compound heterozygous mice *Abcc6*$^{+/-}$*; Enpp1*$^{+/asj}$ demonstrated extensive mineralization to essentially the same extent as the corresponding homozygous mutant mice. Thus, deletion of one *Abcc6* allele on the background of *Enpp1* haploinsufficiency is adequate to cause ectopic mineralization, suggesting the presence of digenic, synergistic consequences of mutations in the genes involved in the control of mineral deposition. In this context, it is of interest to note that a human family with a heterozygous *ABCC6* mutation in one allele and a heterozygous *GGCX* mutation in the other allele has been shown to demonstrate ectopic mineralization in the skin with cutaneous manifestations consistent with PXE (40). Thus, synergistic gene defects in the complex mineralization/anti-mineralization networks, compounded by factors such as diet, can profoundly modulate the degree of ectopic tissue mineralization in processes like nephrocalcinosis.

Supplementary Material

Refer to Web version on PubMed Central for supplementary material.

ACKNOWLEDGEMENTS

The authors thank the following individuals: Adele Donahue, Haitao Guo and Dian Wang for animal care and laboratory assistance; Mark Pawlowski for histopathology; Neil Mehta and Madhukar Thakur for CT imaging, and Andrzej Fertala in polarizing microscopy - all at Jefferson Medical College. Jamie Ford at Penn Regional Nanotechnology Facility, University of Pennsylvania, assisted in EDAX analysis. Carol Kelly assisted in manuscript preparation. This study was supported by NIH/NIAMS grants R01AR28450 and R01AR55225.

Abbreviations

GACI	generalized arterial calcification of infancy
PXE	pseudoxanthoma elasticum

REFERENCES

1. Li Q, Uitto J. Mineralization/anti-mineralization networks in the skin and vascular connective tissues. Am J Pathol. 2013; 183:10–18. [PubMed: 23665350]
2. Vervaet BA, Verhulst A, D'Haese PC, De Broe ME. Nephrocalcinosis: new insights into mechanisms and consequences. Nephrology, dialysis, transplantation : official publication of the European Dialysis and Transplant Association - European Renal Association. 2009; 24(7):2030–2035.
3. Khan SR. Nephrocalcinosis in animal models with and without stones. Urol Res. 2010; 38(6):429–438. [PubMed: 20658131]
4. Cochat P, Hulton SA, Acquaviva C, et al. Primary hyperoxaluria Type 1: indications for screening and guidance for diagnosis and treatment. Nephrology, dialysis, transplantation : official publication of the European Dialysis and Transplant Association - European Renal Association. 2012; 27(5): 1729–1736.
5. Hoppe B, Leumann E, von Unruh G, Laube N, Hesse A. Diagnostic and therapeutic approaches in patients with secondary hyperoxaluria. Frontiers in bioscience : a journal and virtual library. 2003; 8:e437–e443. [PubMed: 12957811]
6. Uitto J, Li Q, Jiang Q. Pseudoxanthoma elasticum: molecular genetics and putative pathomechanisms. J Invest Dermatol. 2010; 130:661–670. [PubMed: 20032990]
7. Uitto J, Varadi A, Bercovitch L, Terry PF, Terry SF. Pseudoxanthoma elasticum: progress in research toward treatment: summary of the 2012 PXE International Research Meeting. J Invest Dermatol. 2013; 133:1444–1449. [PubMed: 23673496]
8. Gheduzzi D, Sammarco R, Quaglino D, et al. Extracutaneous ultrastructural alterations in pseudoxanthoma elasticum. Ultrastruct Pathol. 2003; 27(6):375–384. [PubMed: 14660276]
9. Crespi G, Derchi LE, Saffioti S. Sonographic detection of renal changes in pseudoxanthoma elasticum. Urol Radiol. 1992; 13(4):223–225. [PubMed: 1598746]
10. Belinsky MG, Kruh GD. MOAT-E (ARA) is a full-length MRP/cMOAT subfamily transporter expressed in kidney and liver. Br J Cancer. 1999; 80(9):1342–1349. [PubMed: 10424734]
11. Rutsch F, Nitschke Y, Terkeltaub R. Genetics in arterial calcification: pieces of a puzzle and cogs in a wheel. Circ Res. 2011; 109(5):578–592. [PubMed: 21852556]
12. Nitschke Y, Rutsch F. Genetics in arterial calcification: lessons learned from rare diseases. Trends Cardiovasc Med. 2012; 22(6):145–149. [PubMed: 23122642]
13. Ruf N, Uhlenberg B, Terkeltaub R, Nurnberg P, Rutsch F. The mutational spectrum of ENPP1 as arising after the analysis of 23 unrelated patients with generalized arterial calcification of infancy (GACI). Hum Mutat. 2005; 25(1):98. [PubMed: 15605415]
14. Nitschke Y, Baujat G, Botschen U, et al. Generalized arterial calcification of infancy and pseudoxanthoma elasticum can be caused by mutations in either *ENPP1* or *ABCC6*. Am J Hum Genet. 2012; 90(1):25–39. [PubMed: 22209248]

15. Li Q, Brodsky JL, Conlin L, et al. Mutations in the *ABCC6* gene as a cause of generalized arterial calcification of infancy - genotypic overlap with pseudoxanthoma elasticum. J Invest Dermatol. 2013
16. Gorgels TG, Hu X, Scheffer GL, et al. Disruption of *Abcc6* in the mouse: novel insight in the pathogenesis of pseudoxanthoma elasticum. Hum Mol Genet. 2005; 14(13):1763–1773. [PubMed: 15888484]
17. Klement JF, Matsuzaki Y, Jiang QJ, et al. Targeted ablation of the *Abcc6* gene results in ectopic mineralization of connective tissues. Mol Cell Biol. 2005; 25(18):8299–8310. [PubMed: 16135817]
18. Sali, A.; Favaloro, JM.; Terkeltaub, R.; Goding, JW. Germline deletion of the nucleoside triphosphate pyrophosphohydrolase *NTPPPH) plasma cell membrnae glycoprotein-1 (PC-1) produces abnormal calcification of periarticular tissues. In: Vanduffel, LLR., editor. Ecto-ATPases and related ectoenzymes. Maastricht, The Netherlands: Shaker Publishing; 1999. p. 267-282.
19. Okawa A, Nakamura I, Goto S, Moriya H, Nakamura Y, Ikegawa S. Mutation in Npps in a mouse model of ossification of the posterior longitudinal ligament of the spine. Nature Genet. 1998; 19(3):271–273. [PubMed: 9662402]
20. Li Q, Guo H, Chou DW, Berndt A, Sundberg JP, Uitto J. Mutant *Enpp1*^{asj} mouse as a model for generalized arterial calcification of infancy. Disease Models & Mechanisms. 2013; 6:1227–1235. [PubMed: 23798568]
21. Li Q, Uitto J. The mineralization phenotype in *Abcc6 (−/−)* mice is affected by *Ggcx* gene deficiency and genetic background--a model for pseudoxanthoma elasticum. J Mol Med (Berl). 2010; 88(2):173–181. [PubMed: 19784827]
22. Jiang Q, Uitto J. Restricting dietary magnesium accelerates ectopic connective tissue mineralization in a mouse model of pseudoxanthoma elasticum *(Abcc6*$^{-/-}$*)*. Exp Dermatol. 2012; 21:694–699. [PubMed: 22897576]
23. Le Corre Y, Le Saux O, Froeliger F, et al. Quantification of the calcification phenotype of Abcc6-deficient mice with microcomputed tomography. Am J Pathol. 2012; 180(6):2208–2213. [PubMed: 22469843]
24. Kavukcuoglu NB, Li Q, Pleshko N, Uitto J. Connective tissue mineralization in Abcc6(−/−) mice, a model for pseudoxanthoma elasticum. Matrix Biol. 2012; 31:246–252. [PubMed: 22421595]
25. Lomashvili KA, Khawandi W, O'Neill WC. Reduced plasma pyrophosphate levels in hemodialysis patients. J Am Soc Nephrol. 2005; 16(8):2495–2500. [PubMed: 15958726]
26. O'Neill WC, Sigrist MK, McIntyre CW. Plasma pyrophosphate and vascular calcification in chronic kidney disease. Nephrol Dial Transplant. 2010; 25(1):187–191. [PubMed: 19633093]
27. Kirsch AH, Smaczny N, Riegelbauer V, et al. Regulatory T cells improve nephrocalcinosis but not dystrophic cardiac calcinosis in DBA/2 mice. Am J Pathol. 2013; 183(2):382–390. [PubMed: 23746654]
28. Golub EE. Biomineralization and matrix vesicles in biology and pathology. Semin Immunopathol. 2010; 33:409–417. [PubMed: 21140263]
29. Lieske JC, Swift H, Martin T, Patterson B, Toback FG. Renal epithelial cells rapidly bind and internalize calcium oxalate monohydrate crystals. Proc Natl Acad Sci U S A. 1994; 91(15):6987–6991. [PubMed: 8041733]
30. Lieske JC, Norris R, Swift H, Toback FG. Adhesion, internalization and metabolism of calcium oxalate monohydrate crystals by renal epithelial cells. Kidney Int. 1997; 52(5):1291–1301. [PubMed: 9350652]
31. Evan AP, Coe FL, Rittling SR, et al. Apatite plaque particles in inner medulla of kidneys of calcium oxalate stone formers: osteopontin localization. Kidney Int. 2005; 68(1):145–154. [PubMed: 15954903]
32. Hennequin C, Tardivel S, Medetognon J, Drueke T, Daudon M, Lacour B. A stable animal model of diet-induced calcium oxalate crystalluria. Urol Res. 1998; 26(1):57–63. [PubMed: 9537698]
33. Atmani F, Glenton PA, Khan SR. Identification of proteins extracted from calcium oxalate and calcium phosphate crystals induced in the urine of healthy and stone forming subjects. Urol Res. 1998; 26(3):201–207. [PubMed: 9694603]

34. Bates JM, Raffi HM, Prasadan K, et al. Tamm-Horsfall protein knockout mice are more prone to urinary tract infection: rapid communication. Kidney Int. 2004; 65(3):791–797. [PubMed: 14871399]

35. Anderson JC, Williams JC Jr, Evan AP, Condon KW, Sommer AJ. Analysis of urinary calculi using an infrared microspectroscopic surface reflectance imaging technique. Urol Res. 2007; 35(1):41–48. [PubMed: 17205310]

36. Beck L, Karaplis AC, Amizuka N, Hewson AS, Ozawa H, Tenenhouse HS. Targeted inactivation of Npt2 in mice leads to severe renal phosphate wasting, hypercalciuria, and skeletal abnormalities. Proc Natl Acad Sci U S A. 1998; 95(9):5372–5377. [PubMed: 9560283]

37. LaRusso J, Li Q, Jiang Q, Uitto J. Elevated dietary magnesium prevents connective tissue mineralization in a mouse model of pseudoxanthoma elasticum *(Abcc6*$^{-/-}$*)*. J Invest Dermatol. 2009; 129:1388–1394. [PubMed: 19122649]

38. Li Q, Larusso J, Grand-Pierre AE, Uitto J. Magnesium carbonate-containing phosphate binder prevents connective tissue mineralization in *Abcc6*$^{-/-}$ mice-potential for treatment of pseudoxanthoma elasticum. Clin Transl Sci. 2009; 2(6):398–404. [PubMed: 20443931]

39. Gorgels TG, Waarsing JH, de Wolf A, ten Brink JB, Loves WJ, Bergen AA. Dietary magnesium, not calcium, prevents vascular calcification in a mouse model for pseudoxanthoma elasticum. J Mol Med (Berl). 2010; 88(5):467–475. [PubMed: 20177653]

40. Li Q, Grange DK, Armstrong NL, et al. Mutations in the *GGCX* and *ABCC6* genes in a family with pseudoxanthoma elasticum-like phenotypes. J Invest Dermatol. 2009; 129(3):553–563. [PubMed: 18800149]

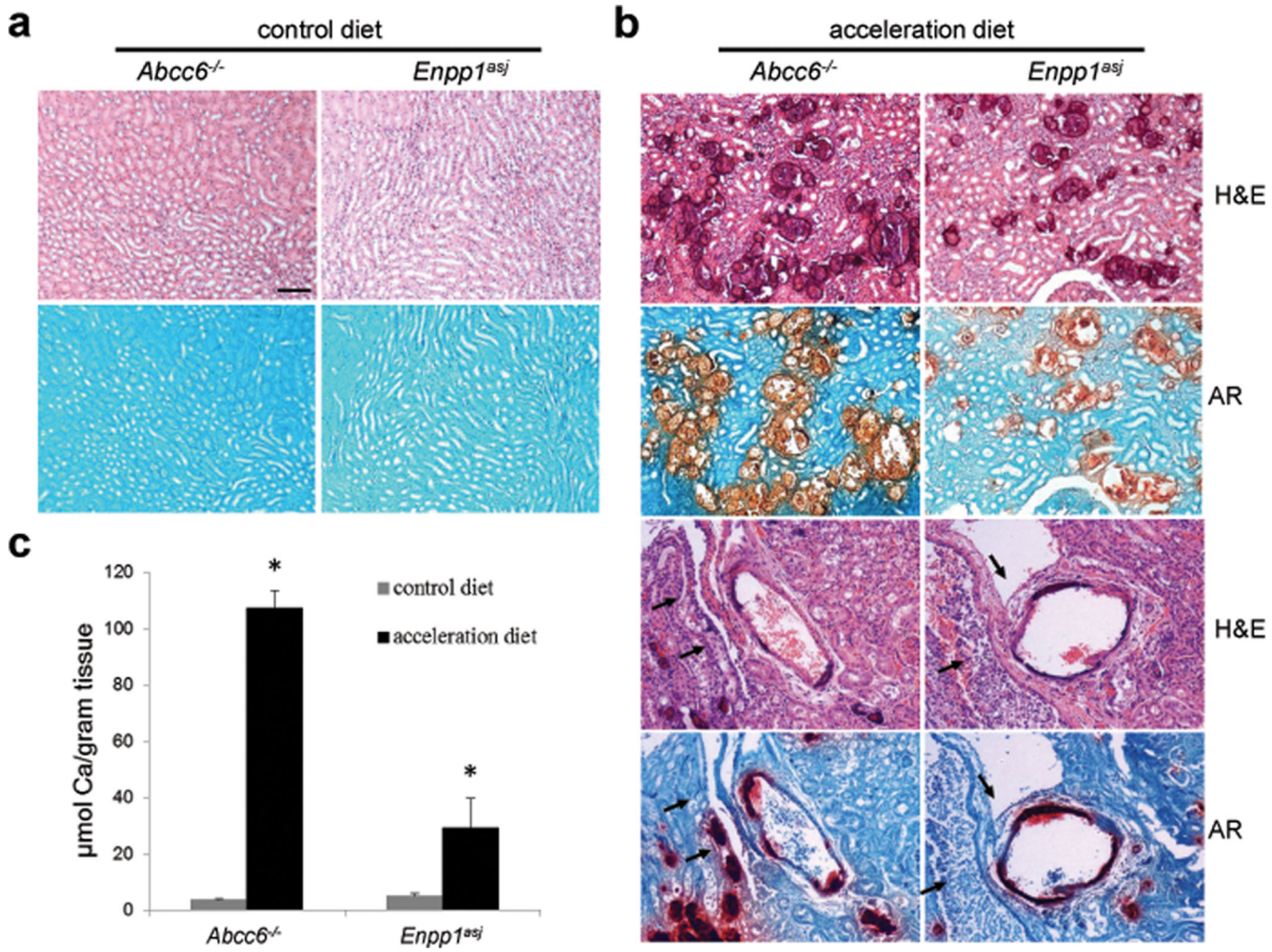

Figure 1. Ectopic mineralization of kidneys in *Abcc6*$^{-/-}$ and *asj* mice placed on acceleration diet

The mice were placed on special diet enriched in phosphate and low in magnesium (for details, see Materials and Methods) at 4 weeks of age and sacrificed at the age of 3 months. For histopathological examination, kidney sections were stained with Hematoxylin and Eosin (HE) and with Alizarin Red (AR) stains. (a) Mice kept on control laboratory diet did not demonstrate ectopic mineralization in the kidneys. (b) The mice on acceleration diet demonstrated extensive mineralization affecting the medullary tubules as well as arcuate and renal arteries (arrows) (scale bar, 100 µm). (c) Chemical assay of the calcium content of renal tissues demonstrated ~30-fold and ~6-fold increases, respectively, in mineralization in *Abcc6*$^{-/-}$ and *asj* mice kept on the acceleration diet *vs.* control diet (*$p<0.001$; n = 5–6 per group).

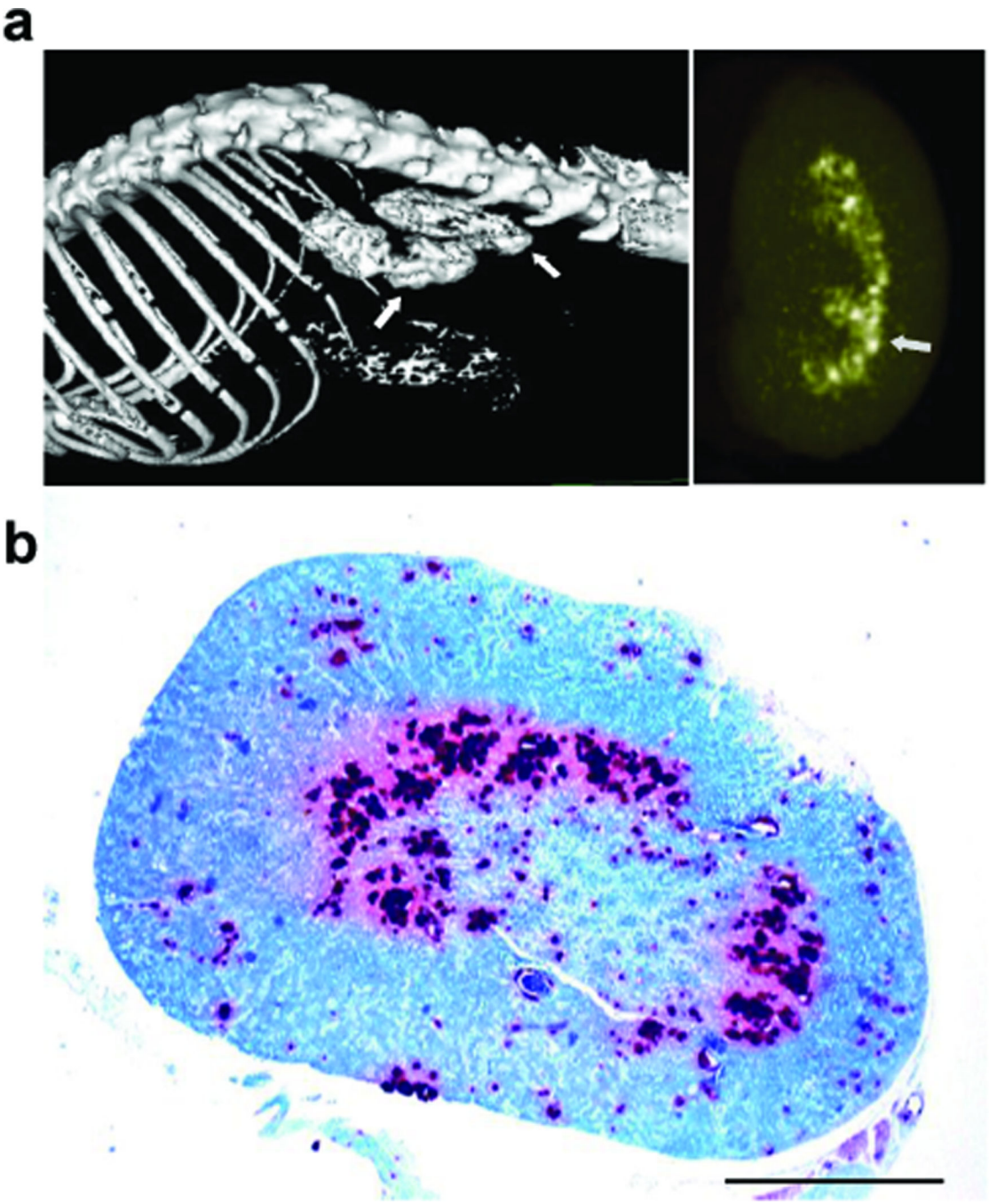

Figure 2. Micro CT imaging and histopathology reveals extensive kidney mineralization in *asj* mice

a) Imaging of the intact mouse (left panel) or isolated kidney *ex vivo* (right panel) reveals ectopic mineralization (arrows). (b) Histopathological staining of transected kidney reveals ectopic mineralization primarily in the medulla, as revealed by Alizarin red stain (scale bar, 10 mm).

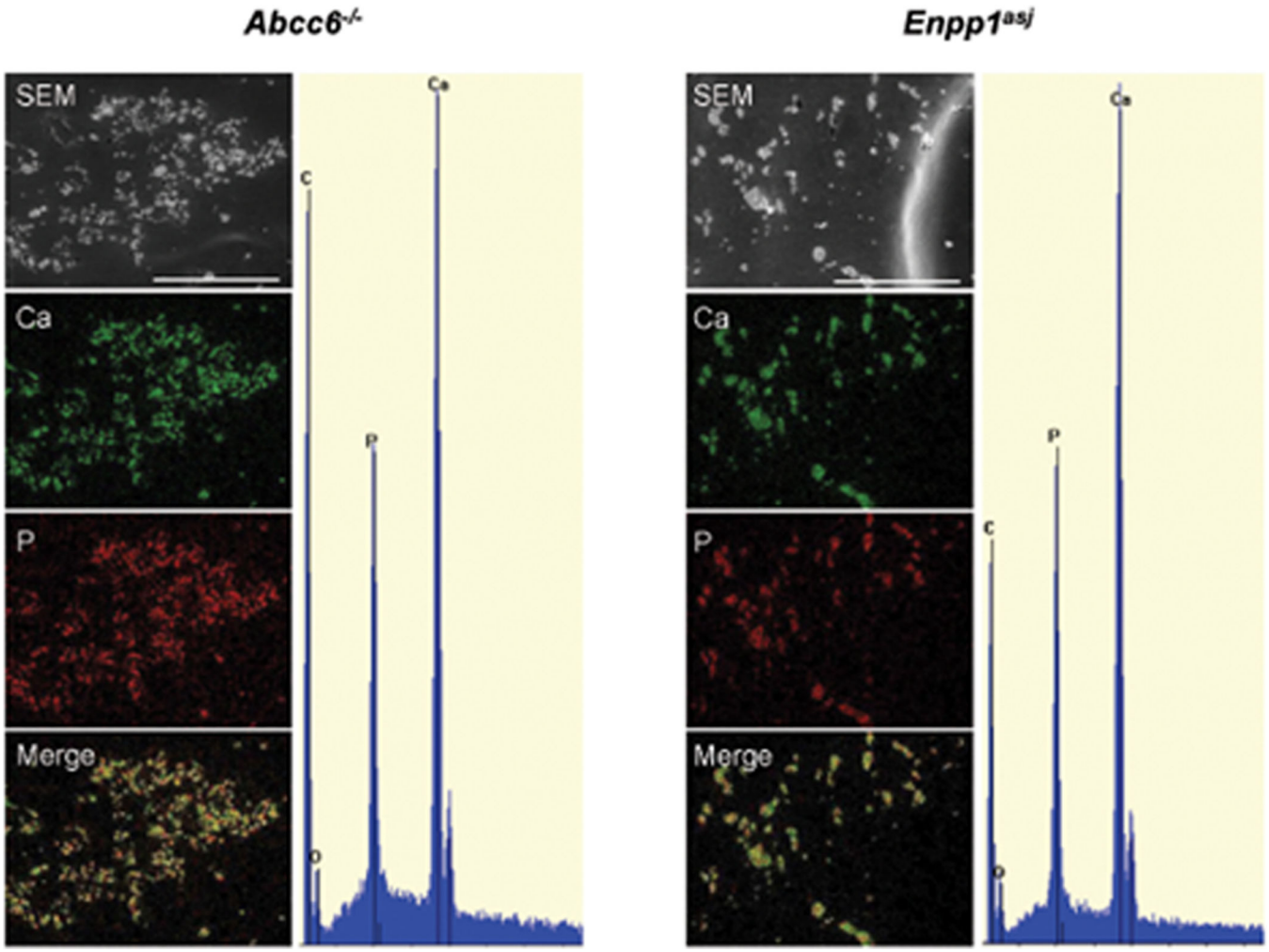

Figure 3. Energy dispersive X-ray analysis of the mineral deposits in the kidney of *Abcc6*$^{-/-}$ and *asj* mice

The results revealed the presence of calcium and phosphorus as the principal ions in ~2:1 ratio. Topographic RADAR mapping of calcium (Ca) and phosphorus (P) revealed co-localization in merged images (scale bar, 1 mm).

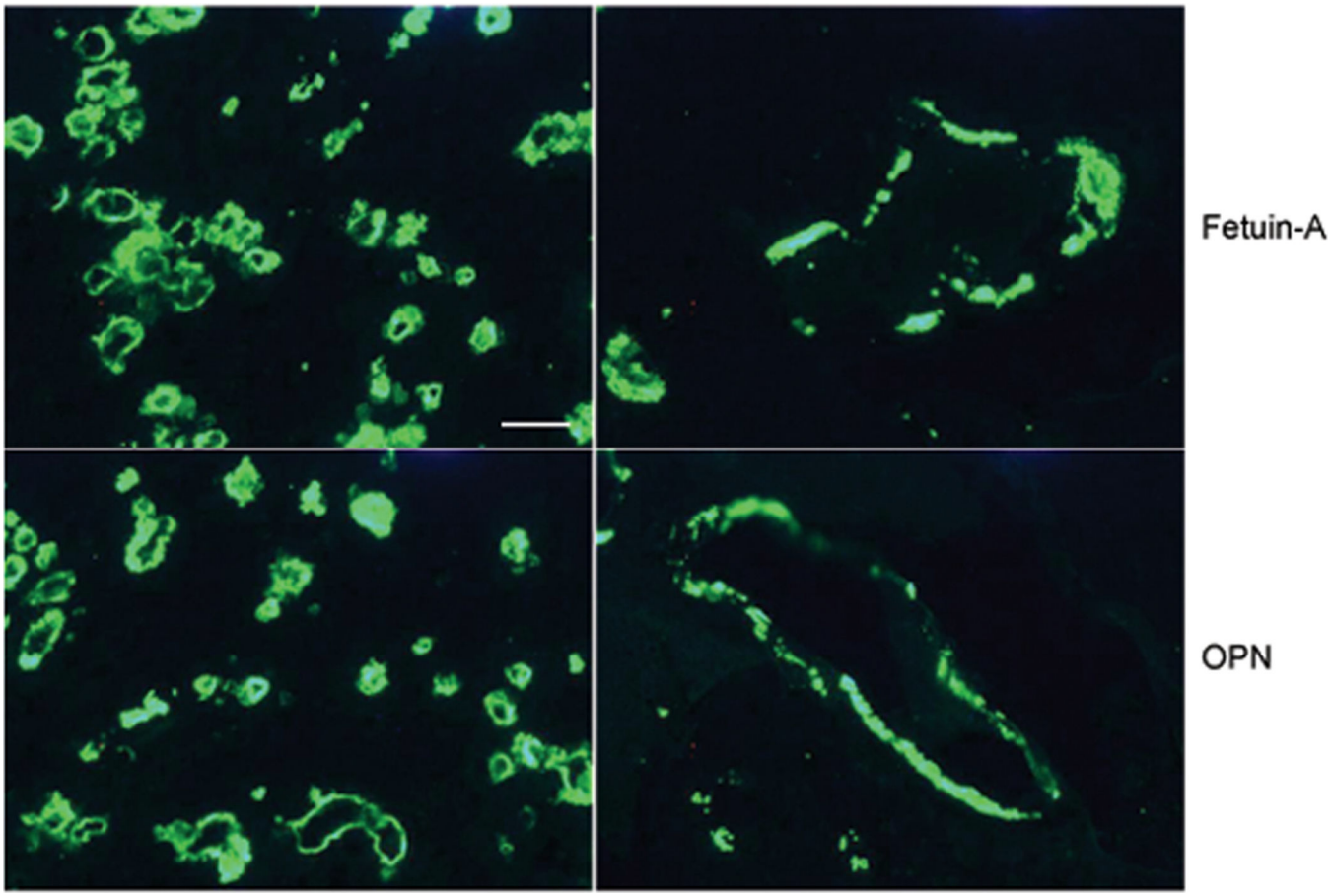

Figure 4. Immunofluorescence of the mineral deposits with antibodies for fetuin-A (upper panels) and for osteopontin (OPN) (lower panels

These two mineralization-associated proteins were found juxtaposed to the mineral deposits (scale bar, 100 μm).

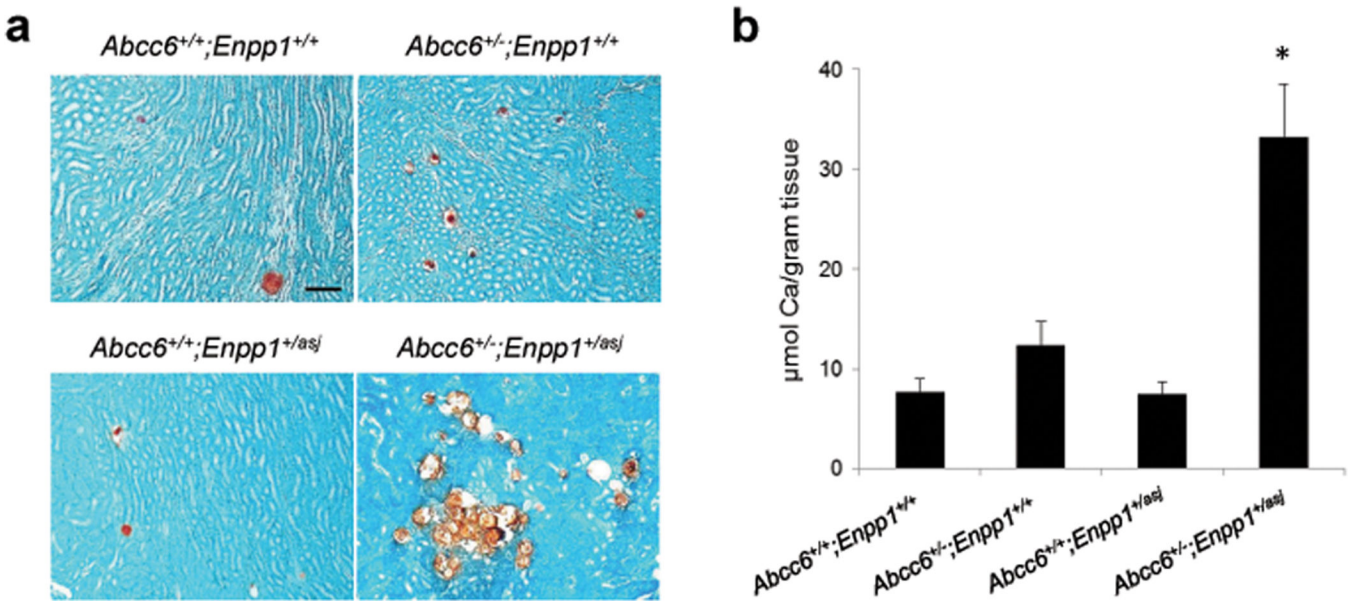

Figure 5. Genetic modulation of nephrocalcinosis

a) Wild-type *Abcc6*$^{+/+}$*; Enpp1*$^{+/+}$ mice, as well as heterozygous *Abcc6*$^{+/-}$ and *Enpp1*$^{+/asj}$ mice on the same background were placed on acceleration diet at 4 weeks of age and kidney mineralization was examined by Alizarin Red stain at 7 months of age. Few foci of ectopic mineralization were noted. However, compound heterozygous mice, *Abcc6*$^{+/-}$*; Enpp1*$^{+/asj}$ demonstrated extensive ectopic mineralization, similar to that noted in the respective homozygous mutant mice (see Fig. 1b). (b) Enhanced mineral deposition in the latter mice was also demonstrated by chemical assay of calcium in the renal tissues (*$p<0.001$ as compared to wild-type and heterozygous mice; n = 8–12 per group; scale bar, 100 µm).

Table 1

Blood parameters of mice on acceleration diet*

Parameter	Concentration (mean ± S.E.)			
	***Abcc6*$^{+/+}$*;Enpp1*$^{+/+}$ (n=8)**	***Abcc6*$^{+/-}$*;Enpp1*$^{+/+}$ (n=9)**	***Abcc6*$^{+/+}$*;Enpp1*$^{+/asj}$ (n=12)**	***Abcc6*$^{+/-}$*;Enpp1*$^{+/asj}$ (n=9)**
Calcium (mg/dL)	10.97 ± 0.25	10.16 ± 0.05	10.30 ± 0.26	10.98 ± 0.20
Phosphorus (mg/dL)	7.83 ± 0.29	7.47 ± 0.59	7.55 ± 0.56	7.76 ± 0.33
Ca/P ratio	1.41 ± 0.06	1.44 ± 0.12	1.45 ± 0.11	1.47 ± 0.05
PP_i (μM)	9.22 ± 1.97	8.36 ± 1.50	9.40 ± 2.06	9.24 ± 2.69
Urea (mg/dL)	62.88 ± 3.20	68.60 ± 2.17	64.36 ± 3.08	63.11 ± 2.25
Creatinine (mg/dL)	0.52 ± 0.05	0.58 ± 0.04	0.52 ± 0.02	0.50 ± 0.03

*The mice were placed on acceleration diet at 4 weeks of age. Blood samples were collected by cardiac puncture, Ca, P, urea and creatinine concentrations were determined in serum and PP_i levels were measured in heparinized plasma.